

A WIREBASKET PRECONDITIONER FOR THE MORTAR BOUNDARY ELEMENT METHOD

THOMAS FÜHRER AND NORBERT HEUER

ABSTRACT. We present and analyze a preconditioner of the additive Schwarz type for the mortar boundary element method. As a basic splitting, on each subdomain we separate the degrees of freedom related to its boundary from the inner degrees of freedom. The corresponding *wirebasket-type* space decomposition is stable up to logarithmic terms. For the blocks that correspond to the inner degrees of freedom standard preconditioners for the hypersingular integral operator on open boundaries can be used. For the boundary and interface parts as well as the Lagrangian multiplier space, simple diagonal preconditioners are optimal. Our technique applies to quasi-uniform and non-uniform meshes of shape-regular elements. Numerical experiments on triangular and quadrilateral meshes confirm theoretical bounds for condition and MINRES iteration numbers.

1. INTRODUCTION

In recent years, different variants of the non-conforming boundary element method (BEM) have been developed. The underlying boundary integral equation is of the first kind with hypersingular operator. *Non-conformity* refers to the presence of discontinuous basis functions. (Note that, in the case of integral equations of the second kind or first kind equations with weakly-singular operator, conforming basis functions can be discontinuous.) The first paper on non-conforming BEM considers a Lagrangian multiplier to deal with the homogeneous boundary condition on open surfaces [8]. This technique was extended in [9] to domain decomposition approximations, and is usually referred to as *mortar method*. In this paper we study preconditioners for the mortar BEM presented in [9]. These are the first results on preconditioning techniques for linear systems stemming from non-conforming boundary elements.

Our preconditioner is based on a decomposition of the approximation space and choosing locally equivalent bilinear forms. It therefore fits the additive Schwarz framework. There is a large amount of literature on the additive Schwarz method, mainly aiming at finite element systems, see, e.g., [18, 20, 24] for overviews. For additive Schwarz techniques applied to boundary elements dealing with hypersingular operators see, e.g., [11, 23, 26], cf. also [22] for an overview. In particular, [11] considers a wirebasket-oriented splitting. Graded meshes

Date: January 28, 2022.

2010 Mathematics Subject Classification. 65N38, 65N55, 65F08.

Key words and phrases. Non-conforming boundary elements, hypersingular operator, domain decomposition, mortar method, preconditioner, additive Schwarz method.

Acknowledgments: The first author is supported by CONICYT through FONDECYT project 3150012, and the second author by CONICYT through projects FONDECYT 1150056 and Anillo ACT1118 (ANANUM).

on curves, locally refined and anisotropic meshes (on surfaces) have been analyzed, respectively, in [7, 13, 16]. Other variants, also for hypersingular operators, consider overlapping decompositions and multiplicative applications, see, e.g., [25, 17].

In this paper we extend the additive Schwarz technique to mortar boundary elements. In this case, due to the presence of a Lagrangian multiplier, system matrices have a saddle point structure. This structure can be handled by using standard arguments aiming at the minimum residual method (MINRES). More precisely, the spectrum of the system matrix (with or without preconditioner) is being controlled by the spectrum of the main block and the singular values of the off-diagonal block (arising due to the presence of the Lagrangian multiplier), see [27]. A second complication due to the non-conformity of the method is that the bilinear form $a(\cdot, \cdot)$ representing the hypersingular operator is replaced by the weakly singular operator acting on surface differential operators (surface curl). There are no standard preconditioners for this bilinear form. Our strategy is to split the subspace of discontinuous basis functions X_h^1 from the rest of the approximation space X_h . The remainder X_h^0 forms a subspace of the energy space of the hypersingular operator. It turns out that the bilinear form $a(\cdot, \cdot)$ reduces to the standard one of the hypersingular operator when restricted to X_h^0 . In this way, standard preconditioners like the ones mentioned previously can be applied to this block (actually, there are individual blocks associated with each subdomain). Now, the other subspace X_h^1 contains all the basis functions associated to interface or boundary nodes. In domain decomposition terms, it is a wirebasket space and is related with the skeleton (or wirebasket) of a coarse mesh which is formed by the subdomains of the underlying decomposition. In our case, basis functions associated to the boundary of a subdomain Γ_i can be decoupled from the other elements of X_h^1 , they form a subspace $X_{i,1}$. It turns out that the bilinear form $a(\cdot, \cdot)$ restricted to $X_{i,1}$ is spectrally equivalent to a diagonal matrix (a mass matrix related to the boundary of Γ_i). In this way, simple diagonal matrices can be used (for the preconditioner) to reduce the problem of preconditioning the bilinear form $a(\cdot, \cdot) : X_h \times X_h \rightarrow \mathbb{R}$ to the standard one of hypersingular operators on each subdomain. In our numerical examples we will use multilevel diagonal scaling from [7] for these parts.

A priori error analysis for domain-oriented non-conforming boundary elements yields quasi-optimal error estimates which are perturbed by (poly-) logarithmic terms depending on the mesh size, see [3, 8, 9]. These perturbations appear due to the non-existence of a well-defined trace operator in the energy space of hypersingular operators. It is unknown whether estimates of these perturbations are sharp. Naturally, such logarithmic perturbations also appear in the analysis of additive Schwarz preconditioners, at least when considering non-overlapping decompositions. Note that, in our method, we subtract a wirebasket space and this amounts to trace operations at the boundaries of subdomains. Also in the case of finite elements, such splitting operations cause logarithmic perturbations, see, e.g., [5]. Eventually, our main result considers combinations of simple diagonal and multilevel diagonal preconditioners and proves that they are optimal up to poly-logarithmic terms. In some cases, logarithmic perturbations of condition number bounds can be optimized by multiplying terms of the preconditioner by different logarithmic weights, see again, e.g., [5]. In this paper we consider three different weightings (*Cases 1, 2, 3*) where *Cases 2, 3* are optimized to show a bound $O(|\log(\underline{h})|^4)$ for the condition number of the preconditioned system. Here, \underline{h} denotes the minimum of the diameters of all elements. In contrast, for *Case 1* (which does not use logarithmic weights for the parts dealing with the bilinear form $a(\cdot, \cdot)$) the theoretical

bound is $O(|\log(h)|^5)$, worse than the bounds for *Cases 2,3*. Our numerical experiments, on the other hand, indicate that *Case 1* is superior to *Cases 2,3*. This suggests that some of the theoretical bounds used for the analysis are not sharp, at least in the particular situation of our numerical examples.

An outline of the remainder of this paper is as follows. In the next section we present the model problem, recall the definition of some Sobolev norms, and present a mortar discretization for the model problem. In Section 3 we recall some results on the MINRES method, present our subspace decompositions and corresponding preconditioners, and state the main result (Theorem 9). Proofs are given in Section 3.3. Some numerical experiments are reported in Section 4. They all confirm our theoretical estimates from Theorem 9, though exhibit smaller logarithmic perturbations than predicted. In particular, we also study the case of locally refined meshes driven by adaptivity, where preconditioners behave as expected. Let us note that we do not know of any a posteriori error analysis for mortar boundary elements. The only known results concerning non-conforming BEM consider two-level (or $h - h/2$) estimators applied to the Nitsche coupling [4], not the mortar coupling.

Notation. We abbreviate estimates of the form $A \leq C \cdot B$ with some constant $C > 0$ by $A \lesssim B$. In particular, we use this notation if C is independent of the mesh size and the number of elements. Analogously, we use $A \gtrsim B$ for $A \geq C \cdot B$. If both $A \lesssim B$ and $A \gtrsim B$ hold true, we use the notation $A \simeq B$. Moreover, $|x|$ denotes the Euclidean norm for a point $x \in \mathbb{R}^3$.

2. MORTAR BOUNDARY ELEMENTS

In this section we briefly recall some results on the mortar boundary element method.

2.1. Model problem and functional analytic setting. Let $\Gamma \subset \mathbb{R}^2 \times \{0\}$ denote a plane open surface with polygonal boundary $\partial\Gamma$. For simplicity we refer to Γ as a domain in \mathbb{R}^2 .

We recall some definitions of Sobolev spaces. Let $S \subset \mathbb{R}^2$ be a bounded subset and define for $0 < s < 1$ the seminorm

$$|u|_{H^s(S)}^2 := \int_S \int_S \frac{|u(x) - u(y)|^2}{|x - y|^{2(s+1)}} dx dy.$$

Then, $H^s(S)$ is equipped with the norm

$$\|u\|_{H^s(S)}^2 := \|u\|_{L^2(S)}^2 + |u|_{H^s(S)}^2,$$

and $\tilde{H}^s(S)$ is defined as the completion of $C_0^\infty(S)$ with respect to the norm

$$\|u\|_{\tilde{H}^s(S)}^2 := |u|_{H^s(S)}^2 + \int_S \frac{|u(x)|^2}{\text{dist}(x, \partial S)^{2s}} dx,$$

where $\text{dist}(x, \partial S) := \inf_{y \in \partial S} |x - y|$. The dual spaces of $H^s(S)$, resp. $\tilde{H}^s(S)$, are denoted by $\tilde{H}^{-s}(S)$, resp. $H^{-s}(S)$. Additionally, $\langle \cdot, \cdot \rangle_S$ denotes the $L^2(S)$ scalar product, which is continuously extended to the duality pairing on $\tilde{H}^{-s}(S) \times H^s(S)$, resp. $H^{-s}(S) \times \tilde{H}^s(S)$.

Let $\mathbf{n} \in \mathbb{R}^3$ denote a normal vector on Γ , e.g., $\mathbf{n} = (0, 0, 1)^T$. Define the hypersingular integral operator (formally) by

$$Wu(x) := -\frac{\partial}{\partial \mathbf{n}_x} \int_{\Gamma} u(y) \frac{\partial}{\partial \mathbf{n}_y} \frac{1}{|y - x|} dy.$$

It is well known that this operator extends to a continuous mapping between $\tilde{H}^{1/2}(\Gamma)$ and $H^{-1/2}(\Gamma)$.

Our model problem reads as follows: Given $f \in L^2(\Gamma)$ we seek for a solution $u \in \tilde{H}^{1/2}(\Gamma)$ such that

$$(1) \quad \langle Wu, v \rangle_{\Gamma} = \langle f, v \rangle_{\Gamma} \quad \forall v \in \tilde{H}^{1/2}(\Gamma).$$

The usual conforming boundary element method consists in replacing $\tilde{H}^{1/2}(\Gamma)$ by a finite-dimensional subspace $\tilde{X}_h \subset \tilde{H}^{1/2}(\Gamma)$ and seeking for a solution $\tilde{u}_h \in \tilde{X}_h$ such that

$$\langle W\tilde{u}_h, \tilde{v}_h \rangle_{\Gamma} = \langle f, \tilde{v}_h \rangle_{\Gamma} \quad \forall \tilde{v}_h \in \tilde{X}_h.$$

In this paper, we study preconditioners for a non-conforming scheme that is based on a decomposition of the surface Γ . In the next section we introduce the corresponding subspace decomposition. The non-conforming method based on this decomposition is called mortar method and is presented in Section 2.3.

2.2. Subspace decomposition and meshes. Let $\Gamma_1, \dots, \Gamma_N$ denote a decomposition into non-intersecting (open) polygonal subdomains giving rise to the coarse mesh

$$\mathcal{T} := \{\Gamma_1, \dots, \Gamma_N\} \quad \text{with} \quad \bar{\Gamma} = \bigcup_{j=1}^N \bar{\Gamma}_j.$$

Each subdomain Γ_i is equipped with (a sequence of) regular and quasi-uniform meshes \mathcal{T}_i . The minimum and maximum diameters of elements of the meshes \mathcal{T}_i are denoted by \underline{h}_i and h_i , respectively. As in [9] we assume without loss of generality that $h_i < 1$ and set

$$\underline{h} := \min_{i=1, \dots, N} \underline{h}_i \quad \text{and} \quad h := \max_{i=1, \dots, N} h_i.$$

Let \mathcal{K}_i denote the set of nodes of \mathcal{T}_i . We will also need the set of interior nodes \mathcal{K}_i^0 and the set of nodes on the boundary of Γ_i , $\mathcal{K}_i^1 := \mathcal{K}_i \setminus \mathcal{K}_i^0$. For a node $z_j \in \mathcal{K}_i$ we denote by $\eta_j^{(i)}$ the (bi)linear basis function which satisfies $\eta_j^{(i)}(z_k) = \delta_{jk}$ for all $z_k \in \mathcal{K}_i$. Introducing the space of piecewise (bi)linear functions

$$X_{h,i} := \{v \in C^0(\Gamma_i) : v = \sum_{z_j \in \mathcal{K}_i} \alpha_j \eta_j^{(i)} \text{ with } \alpha_j \in \mathbb{R}\}$$

we define the product spaces

$$X_h := \prod_{i=1}^N X_{h,i} \subset H^{1/2}(\mathcal{T}) := \prod_{i=1}^N H^{1/2}(\Gamma_i).$$

We denote the respective degrees of freedom by $K_i := \#\mathcal{K}_i = \dim(X_{h,i})$ and $K := \sum_{i=1}^N K_i = \dim(X_h)$. Note that by definition of \mathcal{K}_i , elements of X_h do not necessarily satisfy the homogeneous boundary condition on $\partial\Gamma$ nor continuity across interfaces $\partial\Gamma_i \cap \partial\Gamma_j$.

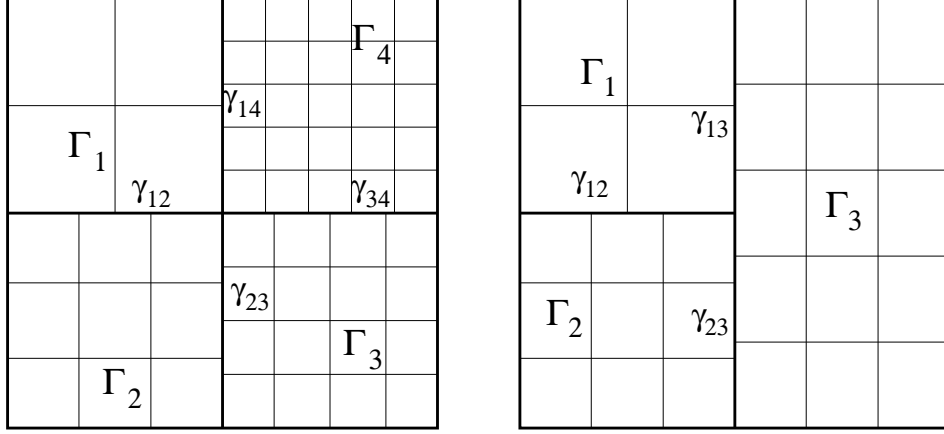


FIGURE 1. Subspace decompositions with non-conforming meshes.

For the mortar BEM, we denote the interface of two neighboring subdomains $\Gamma_i \neq \Gamma_j$ by $\gamma_{ij} := \text{int}(\bar{\Gamma}_i \cap \bar{\Gamma}_j)$ where “int” refers to the (relative) interior. Also, let $\text{diam}(S)$ denote the diameter of a set $S \subseteq \mathbb{R}^3$. We will need the following assumption.

Assumption 1. *Each non-empty interface γ_{ij} ($i, j = 1, \dots, N$, $i \neq j$) consists of an entire edge of Γ_i or Γ_j . If $\text{diam}(\partial\Gamma \cap \partial\Gamma_i) > 0$, then $\partial\Gamma \cap \partial\Gamma_i$ is a union of edges of Γ_i .*

Figure 1 shows examples of two different subspace decompositions with non-conforming meshes. Given the skeleton

$$\gamma := \bigcup_{i=1}^N \partial\Gamma_i,$$

we infer from Assumption 1 that γ is covered by a set of non-intersecting interface edges and boundary edges

$$\tau := \{\gamma_1, \dots, \gamma_L\} \quad \text{with} \quad \bar{\gamma} = \bigcup_{\ell=1}^L \bar{\gamma}_\ell.$$

For each interface edge γ_ℓ , let $\ell_{\text{lag}} \in \{1, \dots, N\}$ resp. $\ell_{\text{mor}} \in \{1, \dots, N\}$ denote the indices of the subdomains $\Gamma_{\ell_{\text{lag}}}$ resp. $\Gamma_{\ell_{\text{mor}}}$ such that

$$\gamma_\ell = \gamma_{\ell_{\text{lag}}, \ell_{\text{mor}}} \quad \text{and} \quad \gamma_\ell \text{ is an edge of } \Gamma_{\ell_{\text{lag}}}.$$

In particular, we set $\ell_{\text{lag}} := i$ if γ_ℓ is a boundary edge, i.e., $\gamma_\ell \subseteq \partial\Gamma_i \cap \partial\Gamma$ so that we can handle the homogeneous boundary conditions and the interface conditions simultaneously.

On each γ_ℓ we introduce a mesh τ_ℓ such that the following assumption is satisfied.

Assumption 2. *The mesh τ_ℓ of γ_ℓ is a strict coarsening of $\mathcal{T}_{\ell_{\text{lag}}} \big|_{\gamma_\ell}$. In particular, any element of τ_ℓ covers at least two elements of $\mathcal{T}_{\ell_{\text{lag}}} \big|_{\gamma_\ell}$.*

Moreover, the diameters of the elements in τ_ℓ and $\mathcal{T}_{\ell_{\text{lag}}} \big|_{\gamma_\ell}$ are comparable, i.e., there exists a constant $C > 0$ such that

$$C^{-1} \text{diam}(t) \leq \text{diam}(T) \leq \text{diam}(t) \quad \text{for all } t \in \tau_\ell \text{ and } T \in \mathcal{T}_{\ell_{\text{lag}}} \big|_{\gamma_\ell} \text{ with } T \subset t.$$

The constant $C > 0$ is independent of ℓ .

We also define the discrete spaces on edges,

$$Y_{h,\ell} := \{\psi \in L^2(\gamma) : \psi|_t \text{ is constant for all } t \in \tau_\ell\}, \quad \ell = 1, \dots, L,$$

and the (global) space for the Lagrangian multiplier

$$Y_h := \prod_{\ell=1}^L Y_{h,\ell}.$$

Based on the previous definitions of decompositions, meshes, and subspaces, we next introduce the mortar boundary element method.

2.3. Mortar BEM. Let $v = (v_1, \dots, v_N)$ with sufficiently smooth component functions v_j defined on Γ_j . We define the piecewise differential operator \mathbf{curl}_H by

$$\mathbf{curl}_H v := \sum_{i=1}^N (\mathbf{curl}_{\Gamma_i} v_i)^0 \quad \text{with} \quad \mathbf{curl}_{\Gamma_i} v_i = (\partial_y v_i(x, y), -\partial_x v_i(x, y), 0)$$

and $(\cdot)^0$ being the extension by 0 onto Γ .

We need the single layer integral operator

$$V\Phi(x) := \int_{\Gamma} \frac{\Phi(y)}{|x - y|} dy,$$

which extends to a continuous operator, mapping $\widetilde{\mathbf{H}}_t^{-1/2}(\Gamma)$ to $\mathbf{H}_t^{1/2}(\Gamma)$. Here

$$\mathbf{H}_t^{1/2}(\Gamma) := \{(v_1, v_2, v_3) \in (H^{1/2}(\Gamma))^3 : v_3 = 0\}$$

and $\widetilde{\mathbf{H}}_t^{-1/2}(\Gamma)$ is its dual space. Furthermore, we define the jumps $[v]$ across interface edges γ_ℓ by

$$[v]|_{\gamma_\ell} := \begin{cases} v_{\ell_{\text{lag}}}|_{\gamma_\ell} & \text{if } \gamma_\ell \subset \partial\Gamma, \\ v_{\ell_{\text{lag}}}|_{\gamma_\ell} - v_{\ell_{\text{mor}}}|_{\gamma_\ell} & \text{else.} \end{cases}$$

With the definitions of the bilinear forms

$$\widehat{a}(u, v) := \langle V\mathbf{curl}_H u, \mathbf{curl}_H v \rangle_{\mathcal{T}} := \sum_{i=1}^N \langle V\mathbf{curl}_H u, \mathbf{curl}_{\Gamma_i} v \rangle_{\Gamma_i},$$

$$b(u, \psi) := \langle [v], \psi \rangle_{\mathcal{T}} := \sum_{\ell=1}^L \langle [v], \psi \rangle_{\gamma_\ell}$$

for all $u, v \in H^{1/2+\varepsilon}(\mathcal{T})$ and $\psi \in L^2(\gamma)$ for some $\varepsilon > 0$ and the right-hand-side functional

$$F(v) := \sum_{i=1}^N \langle f, v_i \rangle_{\Gamma_i},$$

we can state the mortar BEM: Find $(u_h, \phi_h) \in X_h \times Y_h$ such that

$$(2) \quad \begin{aligned} \widehat{a}(u_h, v_h) + b(v_h, \phi_h) &= F(v_h), \\ b(u_h, \psi_h) &= 0 \end{aligned}$$

for all $(v_h, \psi_h) \in X_h \times Y_h$. This formulation admits a unique solution.

Theorem 1 ([9, Theorem 2.1]). *Let Assumptions 1–2 hold true. There exists a unique solution $(u_h, \phi_h) \in X_h \times Y_h$ of (2). Assume that the exact solution u of (1) satisfies $u \in \tilde{H}^{1/2+r}(\Gamma)$ for some $r \in (0, 1/2]$. Then, there holds*

$$\|u - u_h\|_{H^{1/2}(\mathcal{T})} \lesssim |\log(\underline{h})|^2 h^r \|u\|_{\tilde{H}^{1/2+r}(\Gamma)}.$$

Remark 2. *The work [9] deals with homogeneous boundary conditions on $\partial\Gamma$. However, the analysis can be generalized to the present situation, see [8] for the case of BEM with Lagrangian multipliers. In particular, [9, Theorem 2.1] holds true if we do not impose homogeneous boundary conditions in X_h .*

We note that the bilinear form $\widehat{a}(\cdot, \cdot)$ is not elliptic due to the fact that piecewise constant functions $c = (c_1, \dots, c_N) \in X_h$ with $c_i \in \mathbb{R}$ are in the kernel of $\mathbf{curl}_H(\cdot)$. Therefore, for our analysis we will use a simple stabilization of $\widehat{a}(\cdot, \cdot)$ which is similar to the one that is often used for hypersingular integral equations on closed surfaces.

Lemma 3. *Let $0 \neq \alpha \in \mathbb{R}$ denote an arbitrary but fixed constant and let $\xi_\ell \in Y_h$ denote the characteristic function on γ_ℓ , i.e., $\xi_\ell|_{\gamma_k} = \delta_{\ell k}$ and define*

$$(3) \quad a(u, v) := \widehat{a}(u, v) + \alpha^2 \sum_{\ell=1}^L b(u, \xi_\ell) b(v, \xi_\ell) \quad \text{for all } u, v \in X_h.$$

Then, the variational equation (2) is equivalent to: Find $(u_h, \phi_h) \in X_h \times Y_h$ such that

$$(4) \quad \begin{aligned} a(u_h, v_h) + b(v_h, \phi_h) &= F(v_h) \\ b(u_h, \psi_h) &= 0 \end{aligned}$$

for all $(v_h, \psi_h) \in X_h \times Y_h$.

Moreover, for $u, v \in X_h$, there holds

$$(5) \quad \|v\|_{H^{1/2}(\mathcal{T})}^2 \lesssim |\log(\underline{h})| a(v, v) \quad \text{and} \quad a(u, v) \lesssim |\log(\underline{h})|^2 \|u\|_{H^{1/2}(\mathcal{T})} \|v\|_{H^{1/2}(\mathcal{T})}.$$

The involved constants do not depend on h .

Proof. To see the equivalence, we note that $b(u_h, \xi_\ell) = 0$ from the second equation of (2) resp. (4), since $\xi_\ell \in Y_h$. Hence, the additional stabilization terms in the definition of $a(\cdot, \cdot)$ always vanish. Note that the solutions (u_h, ψ_h) of (2) and (4) are in fact identical.

The upper bound in (5) follows from the continuity

$$\widehat{a}(u, v) \lesssim |\log(\underline{h})|^2 \|u\|_{H^{1/2}(\mathcal{T})} \|v\|_{H^{1/2}(\mathcal{T})}$$

of $\widehat{a}(\cdot, \cdot)$ (see [9, Lemma 3.9]) and the continuity

$$b(u, \psi) \lesssim |\log(\underline{h})|^{1/2} \|u\|_{H^{1/2}(\mathcal{T})} \|\psi\|_{L^2(\gamma)}$$

of $b(\cdot, \cdot)$ (see [9, Lemma 3.14]), since

$$\sum_{\ell=1}^L b(u, \xi_\ell) b(v, \xi_\ell) \lesssim |\log(\underline{h})| \|u\|_{H^{1/2}(\mathcal{T})} \|v\|_{H^{1/2}(\mathcal{T})} \sum_{\ell=1}^L \|1\|_{L^2(\gamma_\ell)}^2.$$

To derive the lower bound in (5) we note that the analysis from [8] and [9] yields

$$(6) \quad |v|_{H^{1/2}(\mathcal{T})}^2 := \sum_{i=1}^N |v_i|_{H^{1/2}(\Gamma_i)}^2 \lesssim \widehat{a}(v, v) \quad \text{for all } v \in X_h.$$

Moreover, we apply the following result from [9, Proposition 3.5], which comes from a discrete Poincaré-Friedrichs inequality for fractional-order Sobolev spaces proved in [10]: There exists a constant $C > 0$ such that for all $\varepsilon \in (0, 1/2]$ and any $v \in H^{1/2+\varepsilon}(\mathcal{T})$ with $v|_{\partial\Gamma} = 0$ there holds

$$(7) \quad C^{-1} \|v\|_{L^2(\Gamma)}^2 \leq \varepsilon^{-1} |v|_{H^{1/2+\varepsilon}(\mathcal{T})}^2 + \sum_{\substack{\ell \in \{1, \dots, L\}: \\ \gamma_\ell \text{ is interior edge}}} \text{diam}(\gamma_\ell)^{-1-2\varepsilon} \left(\int_{\gamma_\ell} [v] ds \right)^2.$$

Let $\widehat{\Gamma} \supset \Gamma$ denote an extension of Γ with $\partial\Gamma \subset \widehat{\Gamma}$. Moreover, let $\widehat{\mathcal{T}}$ denote a subdomain decomposition of $\widehat{\Gamma}$ with $\mathcal{T} \subset \widehat{\mathcal{T}}$ such that the shape regularities of \mathcal{T} and $\widehat{\mathcal{T}}$ are equivalent. In particular, $\widehat{\mathcal{T}}$ can be chosen such that each boundary edge $\gamma_\ell \subset \partial\Gamma \cap \partial\Gamma_i$ is an interior edge in $\widehat{\mathcal{T}}$. Thus, (7) holds true if we replace Γ , resp. \mathcal{T} , with $\widehat{\Gamma}$, resp. $\widehat{\mathcal{T}}$. For each $v \in H^{1/2}(\mathcal{T})$ we set $\widehat{v}|_{\mathcal{T}} = v$ and $\widehat{v}|_{\widehat{\mathcal{T}} \setminus \mathcal{T}} := 0$. Then, $\widehat{v} \in H^{1/2}(\widehat{\mathcal{T}})$ and $\|\widehat{v}\|_{H^{1/2+\varepsilon}(\widehat{\mathcal{T}})} = \|v\|_{H^{1/2+\varepsilon}(\mathcal{T})}$. We infer that

$$(8) \quad \begin{aligned} \|v\|_{L^2(\Gamma)}^2 &= \|\widehat{v}\|_{L^2(\widehat{\Gamma})}^2 \lesssim \varepsilon^{-1} |\widehat{v}|_{H^{1/2+\varepsilon}(\widehat{\mathcal{T}})}^2 + \sum_{\ell=1}^L \text{diam}(\gamma_\ell)^{-1-2\varepsilon} \left(\int_{\gamma_\ell} [\widehat{v}] ds \right)^2 \\ &= \varepsilon^{-1} |v|_{H^{1/2+\varepsilon}(\mathcal{T})}^2 + \sum_{\ell=1}^L \text{diam}(\gamma_\ell)^{-1-2\varepsilon} b(v, \xi_\ell)^2 \\ &\leq \varepsilon^{-1} |v|_{H^{1/2+\varepsilon}(\mathcal{T})}^2 + C' \alpha^2 \sum_{\ell=1}^L b(v, \xi_\ell)^2 \end{aligned}$$

with some constant $C' > 0$ depending on α and the diameters of γ_ℓ but not on ε . Finally, choosing $\varepsilon = |\log(\underline{h})|^{-1}$, the inverse estimate

$$\underline{h}^\varepsilon |v|_{H^{1/2+\varepsilon}(\mathcal{T})} \lesssim |v|_{H^{1/2}(\mathcal{T})}$$

together with (8) and (6) shows ellipticity of $a(\cdot, \cdot)$. \square

2.4. Discretizations. For real-valued vectors we use bold symbols, e.g., \mathbf{x} . Each vector $\mathbf{x} \in \mathbb{R}^K$ is uniquely associated to a function $v \in X_h$ in the following way. Let

$$\{\eta_1^{(1)}, \dots, \eta_{K_1}^{(1)}, \eta_1^{(2)}, \dots, \eta_{K_2}^{(2)}, \dots, \eta_1^{(N)}, \dots, \eta_{K_N}^{(N)}\}$$

denote the basis of X_h . For simplicity we use the notation η_1, \dots, η_K for the basis. Then, $\mathbf{x} \in \mathbb{R}^K$ (with $K = \sum_{i=1}^N K_i$) corresponds to

$$v = \sum_{i=1}^N \sum_{j=1}^{K_i} \mathbf{x}_{j+\sum_{k=1}^{i-1} K_k} \eta_j^{(i)} = \sum_{j=1}^K \mathbf{x}_j \eta_j.$$

We define the Galerkin matrix $\mathbf{A} \in \mathbb{R}^{K \times K}$ of $a(\cdot, \cdot)$ as

$$\mathbf{A}_{jk} := a(\eta_k, \eta_j) \quad \text{for } j, k = 1, \dots, K.$$

Let $\{\chi_j^{(\ell)}\}$ denote the basis of $Y_{h,\ell}$ with $\chi_j^{(\ell)}|_{t_k} = \delta_{jk}$ for $t_k \in \tau_\ell$. Analogously as before, we write χ_1, \dots, χ_M with $M := \sum_{\ell=1}^L M_\ell := \sum_{\ell=1}^L \#Y_{h,\ell}$ for the corresponding basis of Y_h .

Then, each $\psi \in Y_h$ can be written as

$$\psi = \sum_{j=1}^M \mathbf{y}_j \chi_j \quad \text{for some } \mathbf{y} \in \mathbb{R}^M.$$

We define the matrix $\mathbf{B} \in \mathbb{R}^{M \times K}$ by

$$\mathbf{B}_{jk} := b(\eta_k, \chi_j) \quad j = 1, \dots, M, k = 1, \dots, K.$$

Denoting the right-hand side vector by $\mathbf{f} \in \mathbb{R}^K$ with $\mathbf{f}_k := F(\eta_k)$, the formulation (4) is equivalent to the matrix-vector equation: Find $(\mathbf{x}, \mathbf{y})^T \in \mathbb{R}^{K+M}$ such that

$$\mathbf{C} \begin{pmatrix} \mathbf{x} \\ \mathbf{y} \end{pmatrix} := \begin{pmatrix} \mathbf{A} & \mathbf{B}^T \\ \mathbf{B} & \mathbf{0} \end{pmatrix} \begin{pmatrix} \mathbf{x} \\ \mathbf{y} \end{pmatrix} = \begin{pmatrix} \mathbf{f} \\ \mathbf{0} \end{pmatrix}.$$

3. PRECONDITIONING

In this section we analyze different wirebasket preconditioners for the mortar BEM considered in Section 2. First, we recall results on the MINRES method.

3.1. Minimal residual method. Throughout we consider the preconditioned minimal residual method (MINRES) with inner products $\langle \mathbf{x}, \mathbf{y} \rangle_{\mathbf{P}} := \mathbf{y}^T \mathbf{P} \mathbf{x}$ induced by block-diagonal preconditioners of the form

$$(9) \quad \mathbf{P} = \begin{pmatrix} \mathbf{P}_{\mathbf{A}} & \\ & \mathbf{P}_{\mathbf{B}} \end{pmatrix},$$

where the blocks $\mathbf{P}_{\mathbf{A}} \in \mathbb{R}^{K \times K}$, $\mathbf{P}_{\mathbf{B}} \in \mathbb{R}^{M \times M}$ are symmetric and positive definite. (Here and in the following, empty spaces represent null matrices of appropriate dimensions.) The preconditioned system then reads

$$\mathbf{P}^{-1} \mathbf{C} = \begin{pmatrix} \mathbf{P}_{\mathbf{A}}^{-1} \mathbf{A} & \mathbf{P}_{\mathbf{A}}^{-1} \mathbf{B}^T \\ \mathbf{P}_{\mathbf{B}}^{-1} \mathbf{B} & \end{pmatrix}$$

Furthermore, define the matrix

$$\tilde{\mathbf{C}} := \begin{pmatrix} \tilde{\mathbf{A}} & \tilde{\mathbf{B}}^T \\ \tilde{\mathbf{B}} & \end{pmatrix} := \begin{pmatrix} \mathbf{P}_{\mathbf{A}}^{-1/2} \mathbf{A} \mathbf{P}_{\mathbf{A}}^{-1/2} & \mathbf{P}_{\mathbf{A}}^{-1/2} \mathbf{B}^T \mathbf{P}_{\mathbf{B}}^{-1/2} \\ \mathbf{P}_{\mathbf{B}}^{-1/2} \mathbf{B} \mathbf{P}_{\mathbf{A}}^{-1/2} & \end{pmatrix} = \mathbf{P}^{-1/2} \mathbf{C} \mathbf{P}^{-1/2}.$$

We note that there holds $\text{spec}(\tilde{\mathbf{C}}) = \text{spec}(\mathbf{P}^{-1} \mathbf{C})$ for the respective spectra. Let

$$(10) \quad \Lambda_{\min} \leq \Lambda_{\max} \quad \text{and} \quad \Sigma_1 \leq \dots \leq \Sigma_m$$

denote, respectively, the extremal eigenvalues of $\tilde{\mathbf{A}}$ and the nonzero singular values of $\tilde{\mathbf{B}}$. Of course, they are all positive. We also define the condition number

$$\kappa(\tilde{\mathbf{C}}) := \max\{|\lambda|; \lambda \in \text{spec}(\tilde{\mathbf{C}})\} / \min\{|\lambda|; \lambda \in \text{spec}(\tilde{\mathbf{C}})\}.$$

The following is a well-established result, see, e.g., [27].

Proposition 4. Denote by $\mathbf{r}^{(k)} := \mathbf{P}^{-1}(\mathbf{f} - \mathbf{C}\mathbf{x}^{(k)})$ the residual of the k -th preconditioned MINRES iteration $\mathbf{x}^{(k)}$ with inner product $\langle \cdot, \cdot \rangle_{\mathbf{P}}$. Then there holds

$$\frac{\|\mathbf{r}^{(k)}\|_{\mathbf{P}}^2}{\|\mathbf{r}^{(0)}\|_{\mathbf{P}}^2} \leq 2 \left(\frac{\kappa(\tilde{\mathbf{C}}) - 1}{\kappa(\tilde{\mathbf{C}}) + 1} \right)^k.$$

so that the number of preconditioned MINRES iterations, required to reduce the initial residual to a certain percentage, is bounded by $O(\kappa(\tilde{\mathbf{C}}))$.

Bounds for the spectrum of $\tilde{\mathbf{C}}$ can be specified in terms of the eigenvalues of $\tilde{\mathbf{A}}$ and singular values of $\tilde{\mathbf{B}}$.

Proposition 5 ([19, Lemma 2.1]). *There holds*

$$\begin{aligned} \text{spec}(\mathbf{P}^{-1}\mathbf{C}) \subseteq & [\tfrac{1}{2}(\Lambda_{\min} - \sqrt{\Lambda_{\min}^2 + 4\Sigma_m^2}, \tfrac{1}{2}(\Lambda_{\max} - \sqrt{\Lambda_{\max}^2 + 4\Sigma_1^2})] \\ & \cup [\Lambda_{\min}, \tfrac{1}{2}(\Lambda_{\max} + \sqrt{\Lambda_{\max}^2 + 4\Sigma_m^2})] \end{aligned}$$

with Λ_{\min} , Λ_{\max} , Σ_1 , Σ_m being the numbers from (10).

3.2. Preconditioner and main results. Our preconditioning technique is based on an initial decomposition of X_h into wirebasket components related with the coarse mesh \mathcal{T} and the remainder. Then, individual preconditioners are applied to the three spaces of wirebasket and interior components and the Lagrangian multiplier.

3.2.1. Wirebasket splitting. For the initial decomposition of X_h , we define for each $v_i \in X_{h,i}$ the unique representation

$$(11) \quad v_i = v_{i,1} + v_{i,0} \quad \text{with} \quad v_{i,0} \in X_{i,0} := \{w \in X_{h,i} : w|_{\partial\Gamma_i} = 0\} \text{ and } v_{i,1} := v_i - v_{i,0},$$

and the preconditioning forms $d_j : X_h \times X_h \rightarrow \mathbb{R}$ ($j = 1, 2, 3$) defined by

$$(12a) \quad d_1(u, v) := \sum_{i=1}^N \langle u_{i,1}|_{\partial\Gamma_i}, v_{i,1}|_{\partial\Gamma_i} \rangle_{L^2(\partial\Gamma_i)} + \sum_{i=1}^N \langle W_i u_{i,0}, v_{i,0} \rangle_{\Gamma_i},$$

$$(12b) \quad d_2(u, v) := \sum_{i=1}^N \langle u_{i,1}|_{\partial\Gamma_i}, v_{i,1}|_{\partial\Gamma_i} \rangle_{L^2(\partial\Gamma_i)} + \frac{1}{|\log(\underline{h})|^2} \sum_{i=1}^N \langle W_i u_{i,0}, v_{i,0} \rangle_{\Gamma_i},$$

$$(12c) \quad d_3(u, v) := \sum_{i=1}^N |\log(\underline{h})| \langle u_{i,1}|_{\partial\Gamma_i}, v_{i,1}|_{\partial\Gamma_i} \rangle_{L^2(\partial\Gamma_i)} + \sum_{i=1}^N \langle W_i u_{i,0}, v_{i,0} \rangle_{\Gamma_i}.$$

Here, W_i is the hypersingular integral operator associated with the subdomain Γ_i . Note that, with V_i being the simple-layer integral operator associated with Γ_i , we have

$$\langle V_i \mathbf{curl}_{\Gamma_i} v_{i,0}, \mathbf{curl}_{\Gamma_i} v_{i,0} \rangle_{\Gamma_i} = \langle W_i v_{i,0}, v_{i,0} \rangle_{\Gamma_i} \simeq \|v_{i,0}\|_{\tilde{H}^{1/2}(\Gamma_i)}^2.$$

Definition (12) provides, up to logarithmic terms, stable splittings.

Lemma 6. For all $v \in X_h$ there holds

$$\begin{aligned} |\log(\underline{h})|^{-3}d_1(v, v) &\lesssim a(v, v) \lesssim |\log(\underline{h})|^2d_1(v, v), \\ |\log(\underline{h})|^{-2}d_2(v, v) &\lesssim a(v, v) \lesssim |\log(\underline{h})|^2d_2(v, v), \\ |\log(\underline{h})|^{-3}d_3(v, v) &\lesssim a(v, v) \lesssim |\log(\underline{h})|d_3(v, v). \end{aligned}$$

A proof of Lemma 6 is given in Section 3.3.

3.2.2. Preconditioner for \mathbf{A} . We now consider a preconditioner for the matrix \mathbf{A} that corresponds to the bilinear form $a(\cdot, \cdot)$ on $X_h \times X_h$. Having performed the initial decomposition of X_h into wirebasket and interior components, Lemma 6 and the structure of the bilinear forms d_j defined by (12) show that it suffices to provide preconditioners for the $L^2(\partial\Gamma_i)$ terms and the terms involving the hypersingular integral operator. We use, respectively, a simple diagonal preconditioner and an arbitrary preconditioner for the hypersingular integral operator in the conforming case, see, e.g., [1, 2, 21, 26].

In the following, let \mathbf{P}_{W_i} denote such a preconditioner for the hypersingular integral operator W_i with constants $\lambda_{\min}^{(i)}, \lambda_{\max}^{(i)}$ such that

$$(13) \quad \lambda_{\min}^{(i)} \mathbf{x}^T \mathbf{P}_{W_i} \mathbf{x} \leq \langle W_i v_{i,0}, v_{i,0} \rangle_{\Gamma_i} \leq \lambda_{\max}^{(i)} \mathbf{x}^T \mathbf{P}_{W_i} \mathbf{x}$$

for all $v_{i,0} \in X_{i,0}$ with $v_{i,0} = \sum_{z_j \in \mathcal{K}_i^0} \mathbf{x}_j \eta_j^{(i)}$. Furthermore, let $\mathbf{P}_{\partial\Gamma_i}$ denote a preconditioner with

$$(14) \quad \mu_{\min}^{(i)} \mathbf{y}^T \mathbf{P}_{\partial\Gamma_i} \mathbf{y} \leq \|v_{i,1}\|_{L^2(\partial\Gamma_i)}^2 \leq \mu_{\max}^{(i)} \mathbf{y}^T \mathbf{P}_{\partial\Gamma_i} \mathbf{y}$$

for all $v_{i,1} \in X_{i,1}$ with $v_{i,1} = \sum_{z_j \in \mathcal{K}_i^1} \mathbf{y}_j \eta_j^{(i)}$. Define the preconditioner $\mathbf{P}^{(i)} \in \mathbb{R}^{K_i \times K_i}$ for the i -th subdomain by

$$\mathbf{P}^{(i)} := \begin{cases} \begin{pmatrix} \mathbf{P}_{\partial\Gamma_i} & \\ & \mathbf{P}_{W_i} \end{pmatrix} & \text{if } d_1(\cdot, \cdot) \text{ is used,} \\ \begin{pmatrix} \mathbf{P}_{\partial\Gamma_i} & \\ & |\log(\underline{h})|^{-2} \mathbf{P}_{W_i} \end{pmatrix} & \text{if } d_2(\cdot, \cdot) \text{ is used,} \\ \begin{pmatrix} |\log(\underline{h})| \mathbf{P}_{\partial\Gamma_i} & \\ & \mathbf{P}_{W_i} \end{pmatrix} & \text{if } d_3(\cdot, \cdot) \text{ is used,} \end{cases}$$

and the overall preconditioner $\mathbf{P}_{\mathbf{A}}$ for the matrix \mathbf{A} , corresponding to the bilinear form $a(\cdot, \cdot)$ on X_h , by

$$\mathbf{P}_{\mathbf{A}} := \begin{pmatrix} \mathbf{P}^{(1)} & & \\ & \ddots & \\ & & \mathbf{P}^{(N)} \end{pmatrix}.$$

For the last two definitions we have assumed an appropriate order of the degrees of freedom in $X_{h,i}$. The logarithmic terms in the definition of $\mathbf{P}^{(i)}$ stem from the logarithmic perturbations in the definition (12) of $d_j(\cdot, \cdot)$. In the remainder of this work we will refer to

“Case j ” if $d_j(\cdot, \cdot)$ is used in the definition of $\mathbf{P}_{\mathbf{A}}$ ($j = 1, 2, 3$).

Our main result concerning the preconditioning of \mathbf{A} is as follows.

Theorem 7. *Set*

$$\lambda_{\min} := \min\{\lambda_{\min}^{(1)}, \mu_{\min}^{(1)}, \dots, \lambda_{\min}^{(N)}, \mu_{\min}^{(N)}\} \text{ and } \lambda_{\max} := \max\{\lambda_{\max}^{(1)}, \mu_{\max}^{(1)}, \dots, \lambda_{\max}^{(N)}, \mu_{\max}^{(N)}\}.$$

Then, there holds for all $\mathbf{x} \in \mathbb{R}^K$

$$\begin{cases} |\log(\underline{h})|^{-3} \lambda_{\min} \mathbf{x}^T \mathbf{P}_A \mathbf{x} \lesssim \mathbf{x}^T \mathbf{A} \mathbf{x} \lesssim |\log(\underline{h})|^2 \lambda_{\max} \mathbf{x}^T \mathbf{P}_A \mathbf{x} & \text{for Case 1,} \\ |\log(\underline{h})|^{-2} \lambda_{\min} \mathbf{x}^T \mathbf{P}_A \mathbf{x} \lesssim \mathbf{x}^T \mathbf{A} \mathbf{x} \lesssim |\log(\underline{h})|^2 \lambda_{\max} \mathbf{x}^T \mathbf{P}_A \mathbf{x} & \text{for Case 2,} \\ |\log(\underline{h})|^{-3} \lambda_{\min} \mathbf{x}^T \mathbf{P}_A \mathbf{x} \lesssim \mathbf{x}^T \mathbf{A} \mathbf{x} \lesssim |\log(\underline{h})| \lambda_{\max} \mathbf{x}^T \mathbf{P}_A \mathbf{x} & \text{for Case 3.} \end{cases}$$

Therefore, the condition number of $\tilde{\mathbf{A}}$ is bounded by

$$\kappa(\tilde{\mathbf{A}}) \lesssim |\log(\underline{h})|^\beta \frac{\lambda_{\max}}{\lambda_{\min}}$$

with $\beta = 5$ in Case 1 and $\beta = 4$ in Cases 2,3.

Proof. The proof follows directly from Lemma 6 and Assumptions (13), (14) on the preconditioners. \square

3.2.3. Final preconditioner for the full matrix \mathbf{C} . In order to define the preconditioner \mathbf{P} (9) for the full matrix \mathbf{C} we assume that we have a matrix $\mathbf{P}_B \in \mathbb{R}^{M \times M}$ such that there exist numbers $\sigma_{\min}, \sigma_{\max} > 0$ with

$$(15) \quad \sigma_{\min} \mathbf{y}^T \mathbf{P}_B \mathbf{y} \leq \|\psi\|_{L^2(\gamma)}^2 \leq \sigma_{\max} \mathbf{y}^T \mathbf{P}_B \mathbf{y}$$

for all $\psi = \sum_{m=1}^M \mathbf{y}_m \chi_m \in Y_h$. Below, we will select \mathbf{P}_B to be diagonal with or without logarithmic scaling.

To provide bounds for the spectrum of $\tilde{\mathbf{C}}$ by means of Proposition 5 it remains to bound the singular values $\Sigma_1, \dots, \Sigma_m$ of the matrix $\tilde{\mathbf{B}}$.

Lemma 8. *Let $0 < \Sigma_1 \leq \dots \leq \Sigma_m$ denote the nonzero singular values of the matrix $\tilde{\mathbf{B}}$ and let $\lambda_{\min}, \lambda_{\max}$ be defined as in Theorem 7. Then,*

$$\begin{cases} \lambda_{\min} \sigma_{\min} |\log(\underline{h})|^{-2} \lesssim \Sigma_1^2 \leq \Sigma_m^2 \lesssim \lambda_{\max} \sigma_{\max} & \text{for Case 1,} \\ \lambda_{\min} \sigma_{\min} |\log(\underline{h})|^{-1} \lesssim \Sigma_1^2 \leq \Sigma_m^2 \lesssim \lambda_{\max} \sigma_{\max} & \text{for Case 2,} \\ \lambda_{\min} \sigma_{\min} |\log(\underline{h})|^{-2} \lesssim \Sigma_1^2 \leq \Sigma_m^2 \lesssim \lambda_{\max} \sigma_{\max} |\log(\underline{h})|^{-1} & \text{for Case 3.} \end{cases}$$

A proof of Lemma 8 will be given in Section 3.3.

Now, let $\mathbf{M} \in \mathbb{R}^{M \times M}$ denote the $L^2(\gamma)$ mass matrix, i.e.,

$$\mathbf{M}_{jk} := \langle \chi_j, \chi_k \rangle_\gamma \quad \text{for } j, k = 1, \dots, M.$$

Obviously, \mathbf{M} is diagonal and

$$\|\psi\|_{L^2(\gamma)}^2 = \mathbf{y}^T \mathbf{M} \mathbf{y} \quad \text{for all } \psi = \sum_{m=1}^M \mathbf{y}_m \chi_m \in Y_h.$$

The main result of our paper is the next theorem. Its proof is immediate by combining the previously established estimates, namely Theorem 7 and Lemma 8, together with the general results provided by Propositions 4 and 5.

Theorem 9. *Let $\lambda_{\min}, \lambda_{\max}$ be defined as in Theorem 7 and let $\sigma_{\min}, \sigma_{\max} > 0$ be the numbers from (15). Then the spectrum of the preconditioned matrix has a superset like $\text{spec}(\tilde{\mathbf{C}}) \subseteq [-a, -b] \cup [c, d]$ with numbers $a, b, c, d > 0$ that satisfy the following estimates.*

- Case 1: If $\mathbf{P}_B = |\log(\underline{h})|^{-1}\mathbf{M}$, then $\sigma_{\min} = \sigma_{\max} = |\log(\underline{h})|$ and

$$\lambda_{\min}/\max\{\lambda_{\max}, \lambda_{\max}^{1/2}\}|\log(\underline{h})|^{-3} \lesssim b \leq a \lesssim \lambda_{\max}^{1/2}|\log(\underline{h})|^{1/2},$$

$$\lambda_{\min}|\log(\underline{h})|^{-3} \lesssim c \leq d \lesssim \max\{\lambda_{\max}, \lambda_{\max}^{1/2}\}|\log(\underline{h})|^2.$$

- Case 2: If $\mathbf{P}_B = |\log(\underline{h})|^{-1}\mathbf{M}$, then $\sigma_{\min} = \sigma_{\max} = |\log(\underline{h})|$ and

$$\lambda_{\min}/\max\{\lambda_{\max}, \lambda_{\max}^{1/2}\}|\log(\underline{h})|^{-2} \lesssim b \leq a \lesssim \lambda_{\max}^{1/2}|\log(\underline{h})|^{1/2},$$

$$\lambda_{\min}|\log(\underline{h})|^{-2} \lesssim c \leq d \lesssim \max\{\lambda_{\max}, \lambda_{\max}^{1/2}\}|\log(\underline{h})|^2.$$

- Case 3: If $\mathbf{P}_B = \mathbf{M}$, then $\sigma_{\min} = \sigma_{\max} = 1$ and

$$\lambda_{\min}/\max\{\lambda_{\max}, \lambda_{\max}^{1/2}\}|\log(\underline{h})|^{-3} \lesssim b \leq a \lesssim (\lambda_{\max})^{1/2}|\log(\underline{h})|^{-1/2},$$

$$\lambda_{\min}|\log(\underline{h})|^{-3} \lesssim c \leq d \lesssim \max\{\lambda_{\max}, \lambda_{\max}^{1/2}\}|\log(\underline{h})|.$$

Therefore, the condition number of $\tilde{\mathbf{C}}$ is bounded by

$$\kappa(\tilde{\mathbf{C}}) \lesssim |\log(\underline{h})|^\beta \max\{\lambda_{\max}^{1/2}, \lambda_{\max}^2\}/\lambda_{\min}$$

with $\beta = 5$ in Case 1 and $\beta = 4$ in Cases 2,3. Furthermore, the number of preconditioned MINRES iterations, required to reduce the relative residual to a certain threshold, is bounded like the condition number in the respective case.

3.3. Proofs and technical details. For the proof of Lemma 6 we need a trace inequality and an inverse estimate, which are given in the following two lemmas.

Lemma 10 ([8, Lemma 4.3]). *Let $R \subset \mathbb{R}^2$ be a bounded Lipschitz domain. There exists a constant $C > 0$ such that for all $\varepsilon \in (0, 1/2)$ holds*

$$\|v\|_{L^2(\partial R)} \leq C\varepsilon^{-1/2}\|v\|_{H^{1/2+\varepsilon}(R)} \quad \text{for all } v \in H^{1/2+\varepsilon}(R).$$

Lemma 11 ([12, Lemma 4]). *For a function $v_i \in X_{i,h}$ with splitting (11), $v_i = v_{i,0} + v_{i,1}$, there holds*

$$\|v_{i,0}\|_{\tilde{H}^{1/2}(\Gamma_i)} \lesssim |\log(\underline{h}_i)|\|v_i\|_{H^{1/2}(\Gamma_i)}, \quad i = 1, \dots, N.$$

The proof of [12, Lemma 4] uses [5, Lemma 4.5]. An alternative proof of Lemma 11 which utilizes multilevel norms is given in [14, Theorem 3.6].

Proof of Lemma 6. We start with a proof of the upper bound. Let $v = v^{(0)} + v^{(1)} \in X_h$ with $v_i^{(0)} := v_{i,0}$ and $v_i^{(1)} := v_{i,1}$. Application of the triangle inequality, boundedness (5) of the bilinear form $a(\cdot, \cdot)$, and equivalence $\langle V \cdot, \cdot \rangle_\Gamma \simeq \|\cdot\|_{\tilde{\mathbf{H}}_t^{-1/2}(\Gamma)}^2$ together with the estimate $\|\cdot\|_{\tilde{\mathbf{H}}_t^{-1/2}(\Gamma)} \lesssim \|\cdot\|_{\tilde{\mathbf{H}}_t^{-1/2}(\mathcal{T})}$ for fractional-order Sobolev spaces, leads to

$$\begin{aligned} a(v, v) &\lesssim a(v^{(0)}, v^{(0)}) + a(v^{(1)}, v^{(1)}) \lesssim a(v^{(0)}, v^{(0)}) + |\log(\underline{h})|^2 \|v^{(1)}\|_{H^{1/2}(\mathcal{T})}^2 \\ &\lesssim \sum_{i=1}^N \|\mathbf{curl}_{\Gamma_i} v_{i,0}\|_{\tilde{\mathbf{H}}_t^{-1/2}(\Gamma_i)}^2 + |\log(\underline{h})|^2 \sum_{i=1}^N \|v_{i,1}\|_{H^{1/2}(\Gamma_i)}^2 \end{aligned}$$

Then, $\langle V_i \cdot, \cdot \rangle_{\Gamma_i} \simeq \|\cdot\|_{\widetilde{\mathbf{H}}_t^{-1/2}(\Gamma_i)}^2$ and $\langle V_i \mathbf{curl}_{\Gamma_i} u_{i,0}, \mathbf{curl}_{\Gamma_i} v_{i,0} \rangle_{\Gamma_i} = \langle W_i u_{i,0}, v_{i,0} \rangle_{\Gamma_i}$ for all $u, v \in X_h$ show

$$a(v, v) \lesssim \sum_{i=1}^N \langle W_i v_{i,0}, v_{i,0} \rangle_{\Gamma_i} + |\log(\underline{h})|^2 \sum_{i=1}^N \|v_{i,1}\|_{H^{1/2}(\Gamma_i)}^2.$$

Let $\widetilde{\Gamma}_i$ denote a closed extension of the subdomain Γ_i and let $\widetilde{\mathcal{T}}_i$ denote an extension of the mesh \mathcal{T}_i such that the shape-regularities of the meshes $\widetilde{\mathcal{T}}_i$ and \mathcal{T}_i are equivalent. For $z_j \in \mathcal{K}_i^0$ we set $\widetilde{\eta}_j^{(i)} := \eta_j^{(i)}$ and for $z_j \in \mathcal{K}_i^1$ we define $\widetilde{\eta}_j^{(i)}$ as the (bi-)linear function with $\widetilde{\eta}_j^{(i)}(z_k) = \delta_{jk}$ for all nodes z_k of the mesh $\widetilde{\mathcal{T}}_i$. Hence, $\widetilde{\eta}_j^{(i)}|_{\Gamma_i} = \eta_j^{(i)}$. For an arbitrary function $v_i = \sum_{z_j \in \mathcal{K}_i} \mathbf{x}_j \eta_j^{(i)} \in X_{h,i}$ we define its extension \widetilde{v}_i as

$$\widetilde{v}_i := \sum_{z_j \in \mathcal{K}_i} \mathbf{x}_j \widetilde{\eta}_j^{(i)} \in \widetilde{X}_{h,i}.$$

By the properties of the $H^{1/2}$ - and $\widetilde{H}^{1/2}$ -norms, we have

$$\|v_{i,1}\|_{H^{1/2}(\Gamma_i)}^2 \lesssim \|\widetilde{v}_{i,1}\|_{\widetilde{H}^{1/2}(\widetilde{\Gamma}_i)}^2.$$

Set $\omega_k := \text{supp}(\widetilde{\eta}_k^{(i)})$. We note that there exists a constant $C_{\text{col}} > 0$ that depends only on the shape-regularity of the mesh \mathcal{T}_i such that

$$\|\widetilde{v}_{i,1}\|_{\widetilde{H}^{1/2}(\widetilde{\Gamma}_i)}^2 \leq C_{\text{col}} \sum_{z_k \in \mathcal{K}_i^1} \|\mathbf{x}_k \widetilde{\eta}_k^{(i)}\|_{\widetilde{H}^{1/2}(\omega_k)}^2.$$

With

$$\|\widetilde{\eta}_k^{(i)}\|_{\widetilde{H}^{1/2}(\omega_k)}^2 \simeq \text{diam}(\omega_k) \simeq \|\widetilde{\eta}_k^{(i)}|_{\partial\Gamma_i}\|_{L^2(\omega_k \cap \partial\Gamma_i)}^2 = \|\eta_k^{(i)}|_{\partial\Gamma_i}\|_{L^2(\omega_k \cap \partial\Gamma_i)}^2$$

and the locality of the L^2 -norms we further deduce

$$\|\widetilde{v}_{i,1}\|_{\widetilde{H}^{1/2}(\widetilde{\Gamma}_i)}^2 \lesssim \sum_{z_k \in \mathcal{K}_i^1} \|\mathbf{x}_k \widetilde{\eta}_k^{(i)}\|_{\widetilde{H}^{1/2}(\omega_k)}^2 \lesssim \sum_{z_k \in \mathcal{K}_i^1} \|\mathbf{x}_k \eta_k^{(i)}|_{\partial\Gamma_i}\|_{L^2(\omega_k \cap \partial\Gamma_i)}^2 \simeq \|v_{i,1}|_{\partial\Gamma_i}\|_{L^2(\partial\Gamma_i)}^2.$$

Thus, altogether we have

$$a(v, v) \lesssim \sum_{i=1}^N \langle W_i v_{i,0}, v_{i,0} \rangle_{\Gamma_i} + |\log(\underline{h})|^2 \sum_{i=1}^N \|v_{i,1}|_{\partial\Gamma_i}\|_{L^2(\partial\Gamma_i)}^2,$$

which proves the upper bounds.

For the lower bounds, we use Lemma 10 with $R = \Gamma_i$ and $\varepsilon = |\log(\underline{h})|^{-1}$ (for \underline{h} small enough). Together with an inverse inequality this gives

$$\|v_{i,1}|_{\partial\Gamma_i}\|_{L^2(\partial\Gamma_i)}^2 \lesssim |\log(\underline{h})| \|v_i\|_{H^{1/2}(\Gamma_i)}^2.$$

Using the norm equivalence $\|\cdot\|_{\widetilde{H}^{1/2}(\Gamma_i)}^2 \simeq \langle W_i \cdot, \cdot \rangle_{\Gamma_i}$ and Lemma 11 shows that

$$\langle W_i v_{i,0}, v_{i,0} \rangle_{\Gamma_i} \simeq \|v_{i,0}\|_{\widetilde{H}^{1/2}(\Gamma_i)}^2 \lesssim |\log(\underline{h})|^2 \|v_i\|_{H^{1/2}(\Gamma_i)}^2.$$

Combining the previous relations and summing over $i = 1, \dots, N$ proves

$$\begin{aligned} d_1(v, v) &= \sum_{i=1}^N \langle W_i v_{i,0}, v_{i,0} \rangle_{\Gamma_i} + \sum_{i=1}^N \|v_{i,1}|_{\partial\Gamma_i}\|_{L^2(\partial\Gamma_i)}^2 \leq |\log(\underline{h})|^2 \|v\|_{H^{1/2}(\mathcal{T})}^2, \\ d_2(v, v) &= \sum_{i=1}^N |\log(\underline{h})|^{-2} \langle W_i v_{i,0}, v_{i,0} \rangle_{\Gamma_i} + \sum_{i=1}^N \|v_{i,1}|_{\partial\Gamma_i}\|_{L^2(\partial\Gamma_i)}^2 \leq |\log(\underline{h})| \|v\|_{H^{1/2}(\mathcal{T})}^2, \\ d_3(v, v) &= \sum_{i=1}^N \langle W_i v_{i,0}, v_{i,0} \rangle_{\Gamma_i} + |\log(\underline{h})| \sum_{i=1}^N \|v_{i,1}|_{\partial\Gamma_i}\|_{L^2(\partial\Gamma_i)}^2 \leq |\log(\underline{h})|^2 \|v\|_{H^{1/2}(\mathcal{T})}^2. \end{aligned}$$

Hence, by applying the ellipticity of $a(\cdot, \cdot)$ from Theorem 1, this shows the lower bounds. \square

Proof of Lemma 8. Note that the nonzero singular values of $\tilde{\mathbf{B}}$ are given by the square roots of the eigenvalues of the matrix $\tilde{\mathbf{B}}\tilde{\mathbf{B}}^T$, since $\tilde{\mathbf{B}}$ has full (row) rank. Furthermore, we note that the smallest and largest singular values are given, respectively, by the minimum and maximum of the term

$$\max_{\mathbf{y} \in \mathbb{R}^K} \frac{b(v, \psi)}{\|\mathbf{y}\|_{\mathbf{P}_A} \|\mathbf{x}\|_{\mathbf{P}_B}} \quad \text{with } v = \sum_{k=1}^K \mathbf{y}_k \eta_k \text{ and } \psi = \sum_{m=1}^M \mathbf{x}_m \chi_m.$$

We start with the upper bound. By the Cauchy-Schwarz and triangle inequalities we have

$$b(v, \psi)^2 \leq 2\|\psi\|_{L^2(\gamma)}^2 \sum_{i=1}^N \|v_i\|_{L^2(\partial\Gamma_i)}^2 \leq \|\psi\|_{L^2(\gamma)}^2 |\log(\underline{h})|^{M_j} d_j(v, v)$$

with $M_1 = M_2 = 0$ and $M_3 = -1$. This together with $d_j(v, v) \lesssim \lambda_{\max} \mathbf{y}^T \mathbf{P}_A \mathbf{y}$ and $\|\psi\|_{L^2(\gamma)}^2 \leq \sigma_{\max} \mathbf{x}^T \mathbf{P}_B \mathbf{x}$ from (15) proves the upper bound.

For the lower bound, we use the proof of Lemma 6 to see that

$$\lambda_{\min} \mathbf{y}^T \mathbf{P}_A \mathbf{y} \lesssim d_j(v, v) \lesssim |\log(\underline{h})|^{m_j} \|v\|_{H^{1/2}(\mathcal{T})}^2$$

with $m_1 = m_3 = -2$ and $m_2 = -1$. This leads to the estimate

$$\max_{\mathbf{y} \in \mathbb{R}^K \setminus \{0\}} \frac{b(v, \psi)}{\|\mathbf{y}\|_{\mathbf{P}_A} \|\mathbf{x}\|_{\mathbf{P}_B}} \gtrsim (\lambda_{\min})^{1/2} |\log(\underline{h})|^{-m_j/2} \max_{v \in X_h \setminus \{0\}} \frac{b(v, \psi)}{\|v\|_{H^{1/2}(\mathcal{T})} \|\mathbf{x}\|_{\mathbf{P}_B}}.$$

By using $\|\psi\|_{L^2(\gamma)}^2 \geq \sigma_{\min} \mathbf{x}^T \mathbf{P}_B \mathbf{x}$ from (15) and the discrete *inf-sup* condition

$$\sup_{0 \neq v \in X_h} \frac{b(v, \psi)}{\|v\|_{H^{1/2}(\mathcal{T})}} \geq \beta \|\psi\|_{L^2(\gamma)} \quad \text{for all } \psi \in Y_h$$

from [9, Lemma 3.12] (with constant $\beta > 0$ independent of h) we conclude the lower bound. \square

4. NUMERICAL EXAMPLES

In this section we present numerical examples in which we compare the different behaviors of the preconditioned systems induced by the preconditioning forms $d_1(\cdot, \cdot)$, $d_2(\cdot, \cdot)$, $d_3(\cdot, \cdot)$. Note that block \mathbf{P}_A of the preconditioner \mathbf{P} is determined by the preconditioning forms $d_j(\cdot, \cdot)$. For the second block \mathbf{P}_B we choose, up to a possible logarithmic term, the (diagonal)

mass matrix \mathbf{M} for the Lagrangian multiplier space. We distinguish the following cases (with corresponding numbers $\sigma_{\min}, \sigma_{\max}$ according to Theorem 9, cf. (15)).

$$\begin{aligned} \text{Case 1a)} \quad & \mathbf{P}_{\mathbf{B}} = |\log(\underline{h})|^{-1} \mathbf{M}, & \sigma_{\min} = \sigma_{\max} = |\log(\underline{h})|, \\ \text{Case 1b)} \quad & \mathbf{P}_{\mathbf{B}} = \mathbf{M}, & \sigma_{\min} = \sigma_{\max} = 1, \\ \text{Case 2)} \quad & \mathbf{P}_{\mathbf{B}} = |\log(\underline{h})|^{-1} \mathbf{M}, & \sigma_{\min} = \sigma_{\max} = |\log(\underline{h})|, \\ \text{Case 3)} \quad & \mathbf{P}_{\mathbf{B}} = \mathbf{M}, & \sigma_{\min} = \sigma_{\max} = 1. \end{aligned}$$

Note that *Case 1a*, *Case 2*, *Case 3* correspond to the bounds obtained in Theorem 9, whereas, at least theoretically, we would expect worse bounds for *Case 1b*. Moreover, we compare the results to a simple diagonal preconditioner with

$$(\mathbf{P}_{\mathbf{A}})_{jk} = \mathbf{A}_{jj} \delta_{jk} \text{ and } (\mathbf{P}_{\mathbf{B}})_{jk} = \mathbf{B}_{jj} \delta_{jk},$$

where δ_{jk} denotes the Kronecker delta symbol. In the figures and tables below, we refer to this preconditioner as *diag*.

Throughout, we use the MINRES algorithm, see Section 3.1, to solve the discrete system. We stop the algorithm if the relative residual in the k -th step satisfies

$$\frac{\|\mathbf{r}^{(k)}\|_{\mathbf{P}}}{\|\mathbf{r}^{(0)}\|_{\mathbf{P}}} \leq 10^{-6}.$$

4.1. Diagonal preconditioner and multilevel diagonal preconditioner. For the wirebasket component we use a simple diagonal preconditioner. Indeed, it is straightforward to prove that

$$(16) \quad \|v_{i,1}|_{\partial\Gamma_i}\|_{L^2(\partial\Gamma_i)}^2 \simeq \sum_{z_j \in \mathcal{K}_i^1} \mathbf{y}_j^2 \|\eta_j^{(i)}\|_{L^2(\partial\Gamma_i)}^2 \simeq \sum_{z_j \in \mathcal{K}_i^1} \mathbf{y}_j^2 \text{diam}(\omega_j),$$

where $v_{i,1} = \sum_{z_j \in \mathcal{K}_i^1} \mathbf{y}_j \eta_j^{(i)} \in X_{i,1}$ and $\text{diam}(\omega_j)$ is the diameter of the node patch $\omega_j = \text{supp}(\eta_j^{(i)})$ of z_j . For the example from Section 4.2, we define the diagonal preconditioner

$$(\mathbf{P}_{\partial\Gamma_i})_{jk} := \frac{|\omega_j|^{1/2}}{12} \delta_{jk}.$$

According to (16) it is optimal, that is, the numbers from (14) behave like

$$(17) \quad \mu_{\min}^{(i)} \simeq \mu_{\max}^{(i)} \simeq 1, \quad i = 1, \dots, N.$$

For the example from Section 4.3 we test as preconditioner (for the wirebasket components) the diagonal of the matrix, i.e., we set

$$(\mathbf{P}_{\partial\Gamma_i})_{jk} := \langle V_i \mathbf{curl}_H \eta_k^{(i)}, \mathbf{curl}_H \eta_j^{(i)} \rangle_{\Gamma_i} \delta_{jk}.$$

Since $\langle V_i \mathbf{curl}_H \eta_j^{(i)}, \mathbf{curl}_H \eta_j^{(i)} \rangle_{\Gamma_i} \simeq \text{diam}(\omega_j) \simeq |\omega_j|^{1/2}$ the constants from (14) satisfy (17) in this case as well.

It remains to select preconditioners for the matrix blocks that belong to the interior unknowns, i.e., the ones corresponding to the nodes \mathcal{K}_i^0 , $i = 1, \dots, N$. As indicated by (13), it is enough to take for each subdomain a standard preconditioner that works for the

hypersingular operator. In the following we use as \mathbf{P}_{W_i} a multilevel diagonal preconditioner, i.e.,

$$\mathbf{P}_{W_i}^{-1} := \sum_{\ell_i=0}^{L_i} \mathbf{T}_{\ell_i} \mathbf{D}_{\ell_i}^{-1} \mathbf{T}_{\ell_i}^T.$$

More precisely, we consider $\mathcal{T}_i = \mathcal{T}_{i,L_i}$ as the finest level of a sequence of meshes $\mathcal{T}_{i,\ell}$ ($\ell = 0, \dots, L_i$). Then, \mathbf{D}_{ℓ_i} is the diagonal part of the Galerkin matrix of $\langle V \mathbf{curl}_H(\cdot), \mathbf{curl}_H(\cdot) \rangle_{\Gamma_i}$ with respect to the nodal basis of $X_{i,0}$ on level ℓ_i and \mathbf{T}_{ℓ_i} is the matrix representation of the embedding operator which embeds elements of the space $X_{i,0}$ on a coarse level ℓ_i to functions on the fine level L_i . For the examples from Section 4.2, we replace the entries of $(\mathbf{D}_{\ell_i})_{jj}$ by $|\omega_j^{\ell_i}|^{1/2}/12$. Here, $\omega_j^{\ell_i}$ is the support of the basis functions of level ℓ_i associated with node j .

It is known, see, e.g., [1], that these preconditioners are optimal on triangular meshes, i.e., the constants from (13) satisfy

$$(18) \quad \lambda_{\min}^{(i)} \simeq \lambda_{\max}^{(i)} \simeq 1$$

with mesh size independent constants. Such multilevel preconditioners can be extended to locally refined meshes with assumptions on refinement zones, see, e.g., [1], or by use of special refinement strategies like Newest Vertex Bisection, cf. [7]. The basic idea is that smoothing with the diagonal elements is done with respect to the degrees of freedom, where the associated basis functions have changed.

We remark that the cited results for the multilevel diagonal preconditioners are stated for triangular meshes only. However, for uniform refinements, the same techniques can be used to prove optimality on quadrilateral meshes. Finally, note that (17) and (18) imply that the numbers $\lambda_{\min}, \lambda_{\max}$ from Theorem 7 satisfy

$$\lambda_{\min} \simeq \lambda_{\max} \simeq 1.$$

According to Theorem 9 we then expect bounds $\kappa(\tilde{\mathbf{C}}) = O(|\log \underline{h}|^\beta)$ with $\beta \leq 5$ in *Case 1a* and $\beta \leq 4$ in *Cases 2,3*. A theoretical bound for the condition number in *Case 1b* would result in an exponent $\beta > 5$ (and is not given here). But our numerical results show that this preconditioner is as competitive as in *Case 1a*, and better than in *Cases 2* and *3*. Our explanation is that some of the technical bounds used in proofs are not sharp, see the discussion in the introduction.

4.2. Problem on Z-shaped domain with triangular meshes. We consider the variational formulation (4) with $f = 1$ and stabilization parameter $\alpha = 0.1$ on the Z-shaped domain Γ from Figure 2. In this case we consider only one subdomain, i.e., $\mathcal{T} = \{\Gamma\}$, $N = 1$. The stabilization parameter is chosen such that the lower order stabilization terms in the definition (3) are not the dominating parts in the condition numbers (for large h).

For the definition of the Lagrangian multiplier space Y_h , we combine two adjacent boundary edges to one element of the mesh τ_ℓ . Mesh refinement is driven by Newest Vertex Bisection, see, e.g., [15]. In particular, we note that each triangle T is divided into 4 son elements T_1, \dots, T_4 , with $|T_j| = |T|/4$. Moreover, this refinement rule preserves shape-regularity, i.e.

$$\sup_{T \in \mathcal{T}_\ell} \frac{\text{diam}(T)^2}{|T|} \lesssim \sup_{T \in \mathcal{T}_0} \frac{\text{diam}(T)^2}{|T|},$$

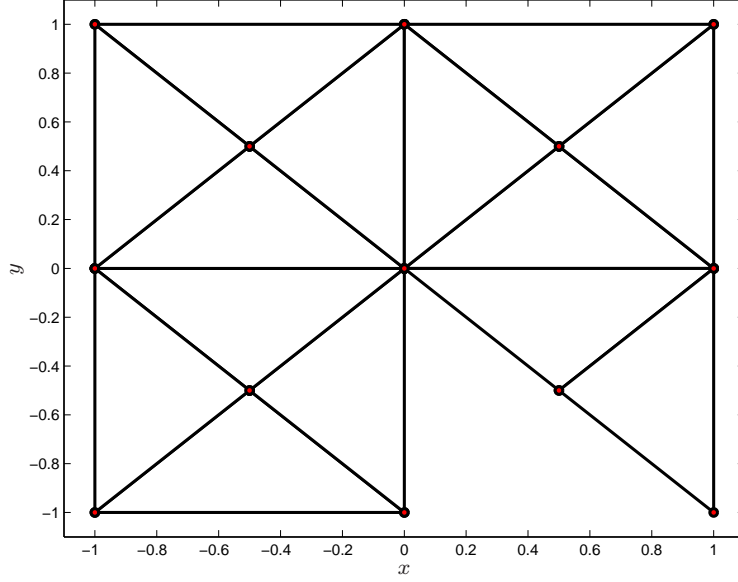


FIGURE 2. Initial triangulation of Z-shaped domain for the example from Section 4.2.

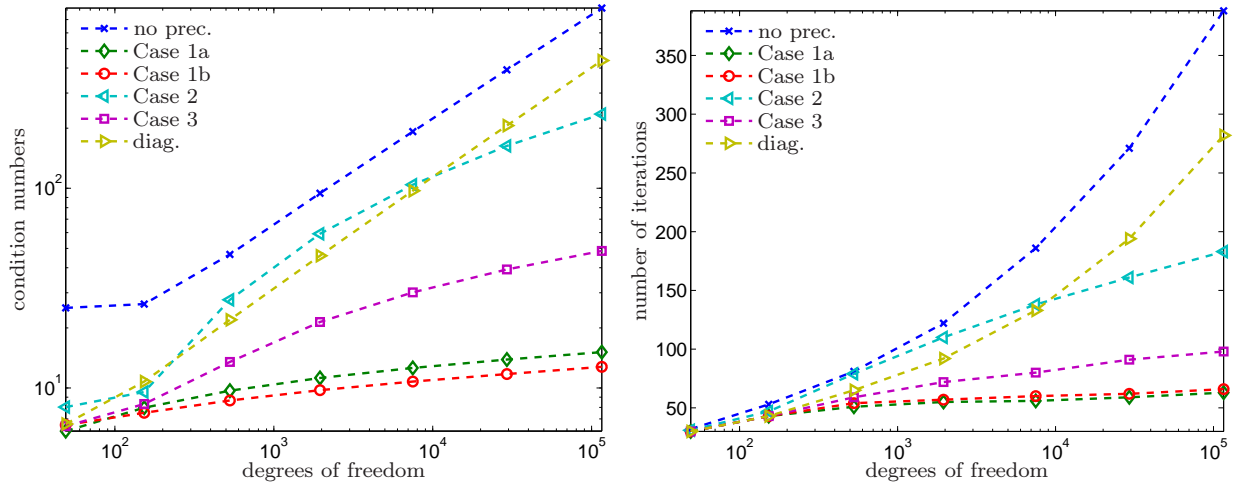


FIGURE 3. Condition numbers of the preconditioned systems and number of iterations in the MINRES algorithm for the example of Section 4.2 and uniform refinements.

which also holds for adaptive mesh refinements. For details we refer the interested reader to [15] and references therein. We remark that the initial triangulation does not satisfy Assumption 2 since, for instance, the boundary edge $(-1, 0) \times \{0\} \times \{0\}$ of \mathcal{T}_0 contains only one boundary element. We use a uniform refinement in the first step, which ensures that Assumption 2 holds true.

Figure 3 shows the condition numbers (left) as well as the numbers of iterations (right) needed to reduce the relative residual in the MINRES method by 10^{-6} in the case of uniform refinements. Additionally, the condition numbers are listed in Table 1.

step	dof	h	\underline{h}	no prec.	1a	1b	2	3	diag.
1	49	1/2	1/2	25.19	6.09	6.52	8.03	6.44	6.60
2	153	1/4	1/4	26.33	7.97	7.51	9.56	8.31	10.77
3	529	1/8	1/8	46.68	9.70	8.66	27.66	13.50	21.95
4	1953	1/16	1/16	94.46	11.22	9.76	59.18	21.41	45.98
5	7489	1/32	1/32	192.36	12.60	10.77	104.18	30.11	97.20
6	29313	1/64	1/64	392.15	13.88	11.75	162.97	39.24	206.00
7	115969	1/128	1/128	799.48	15.12	12.77	235.40	48.56	436.41

TABLE 1. Condition numbers of the preconditioned systems for the example of Section 4.2 and uniform refinements.

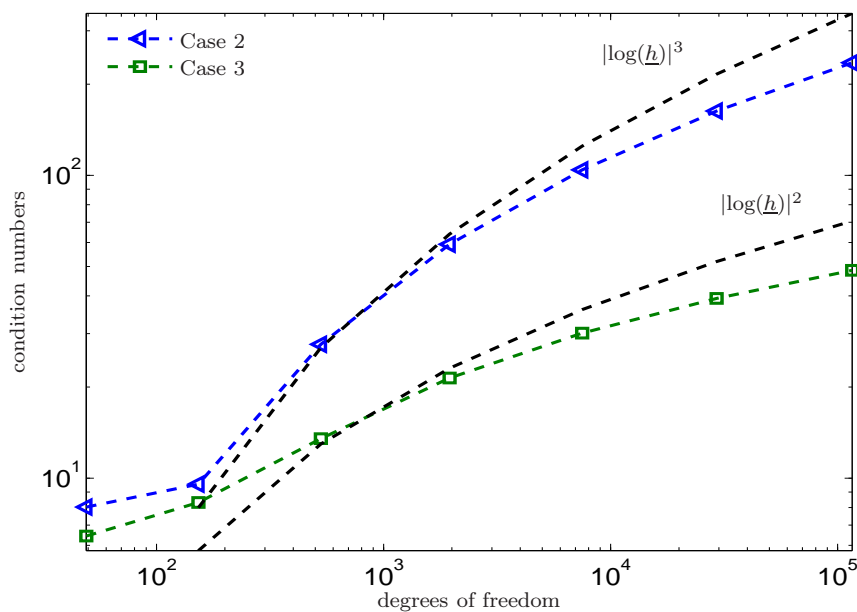


FIGURE 4. Logarithmic behavior of condition numbers for example of Section 4.2 and uniform refinements.

In the following let us refer to P_j as the preconditioner of “*Case j*” ($j \in \{1a, 1b, 2, 3\}$). The numerical results indicate that the preconditioners P_{1a} and P_{1b} are better than the others, and that P_3 is better than P_2 . In contrast, Theorem 9 predicts better bounds for P_2 and P_3 . Nevertheless, all the results confirm the theoretical estimates. Indeed, Figure 4 indicates that $\kappa(\hat{\mathbf{C}})$ is bounded by $O(|\log(\underline{h})|^3)$ even in *Case 2*.

In the next example we consider adaptive mesh refinements, where we use a simple ZZ-type estimator, see, e.g., [6], to mark elements for refinement and additionally refine all elements that share a boundary edge. We note that this estimator is not analyzed in [6] for the present (non-conforming) situation, but is heuristically used to obtain adaptively refined meshes. Condition numbers of the preconditioned systems and numbers of iterations needed in the MINRES algorithm are plotted in Figure 5. Moreover, the condition numbers are listed in Table 2. We observe similar results as in the case of uniform refinements. In

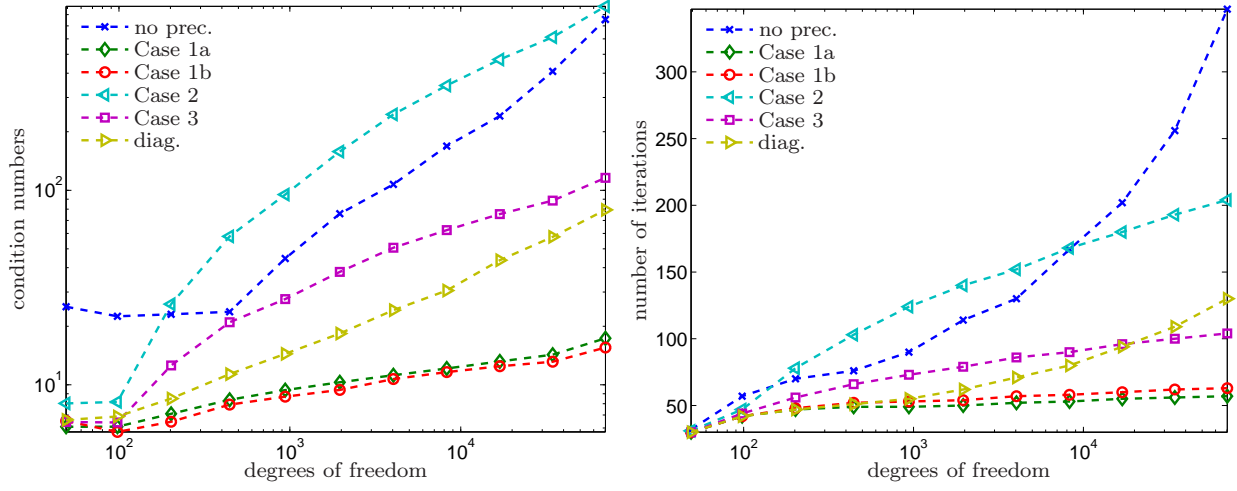


FIGURE 5. Condition numbers of the preconditioned systems and number of iterations in the MINRES algorithm for the example of Section 4.2 and adaptive refinements.

step	dof	h	\underline{h}	no prec.	1a	1b	2	3	diag.
1	49	5.00e-01	1/2	25.19	6.09	6.52	8.03	6.44	6.60
2	98	5.00e-01	1/4	22.51	6.09	5.73	8.17	6.40	6.88
3	202	5.00e-01	1/8	23.05	7.09	6.46	26.00	12.58	8.49
4	444	5.00e-01	1/16	23.74	8.37	7.91	57.98	20.98	11.35
5	939	5.00e-01	1/32	44.60	9.40	8.69	95.06	27.59	14.42
6	1961	3.54e-01	1/64	75.78	10.31	9.42	158.09	38.06	18.36
7	4038	2.50e-01	1/128	107.28	11.21	10.71	245.60	50.67	24.21
8	8289	1.77e-01	1/256	168.65	12.13	11.62	345.67	62.42	30.52
9	16939	1.25e-01	1/512	240.84	13.20	12.46	470.05	75.43	43.72
10	34516	1.25e-01	1/1024	408.58	14.28	13.15	612.52	88.46	57.62
11	70278	8.84e-02	1/2048	755.93	17.34	15.54	882.78	115.87	79.32

TABLE 2. Condition numbers of the preconditioned systems for the example of Section 4.2 and adaptive refinements.

particular, our theoretical results are confirmed also for adaptively refined meshes. Again, the results for the weakest of the domain decomposition preconditioners, P_2 , indicate that $\kappa(\tilde{\mathbf{C}}) \lesssim O(|\log(\underline{h})|^3)$ also in this case, cf. Figure 6.

4.3. Problem with four subdomains and quadrilateral meshes. We consider the variational formulation (4) with $f = 1$ and stabilization parameter $\alpha = 0.1$ on the quadratic domain $\Gamma := (0, 2)^2 \times \{0\}$ with a decomposition into four subdomains $\Gamma_1 = (0, 1)^2 \times \{0\}$, $\Gamma_2 = (1, 2) \times (0, 1) \times \{0\}$, $\Gamma_3 = (0, 1) \times (1, 2) \times \{0\}$, and $\Gamma_4 = (1, 2)^2 \times \{0\}$ sketched in Figure 7. For the intersections $\bar{\Gamma}_1 \cap \bar{\Gamma}_2$ and $\bar{\Gamma}_1 \cap \bar{\Gamma}_3$, we define Γ_1 to be the Lagrangian side and for the intersections $\bar{\Gamma}_4 \cap \bar{\Gamma}_2$ and $\bar{\Gamma}_4 \cap \bar{\Gamma}_3$, we define Γ_4 to be the Lagrangian side. We

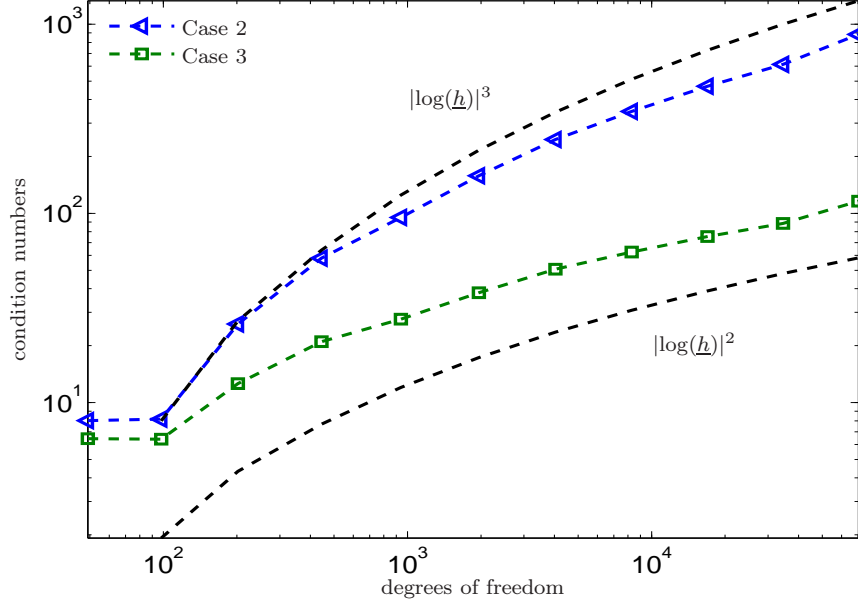


FIGURE 6. Logarithmic behavior of condition numbers for example of Section 4.2 and adaptive refinements.

define the Lagrangian elements that come from Γ_1 and Γ_4 as the union of two adjacent edges that lie in $\partial\Gamma_i$. For the Lagrangian elements that come from Γ_2 and Γ_3 we take the union of three adjacent boundary edges.

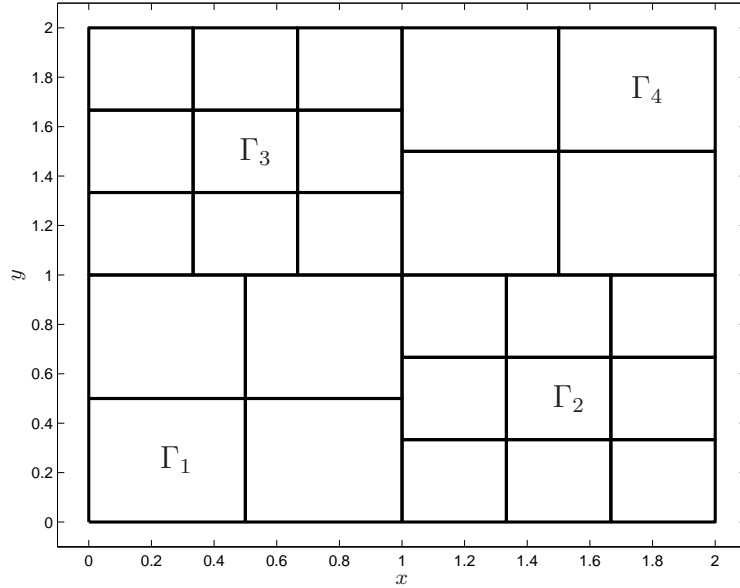


FIGURE 7. Subspace decomposition of $\Gamma = (0, 2)^2 \times \{0\}$ and their initial meshes for the example from Section 4.3.

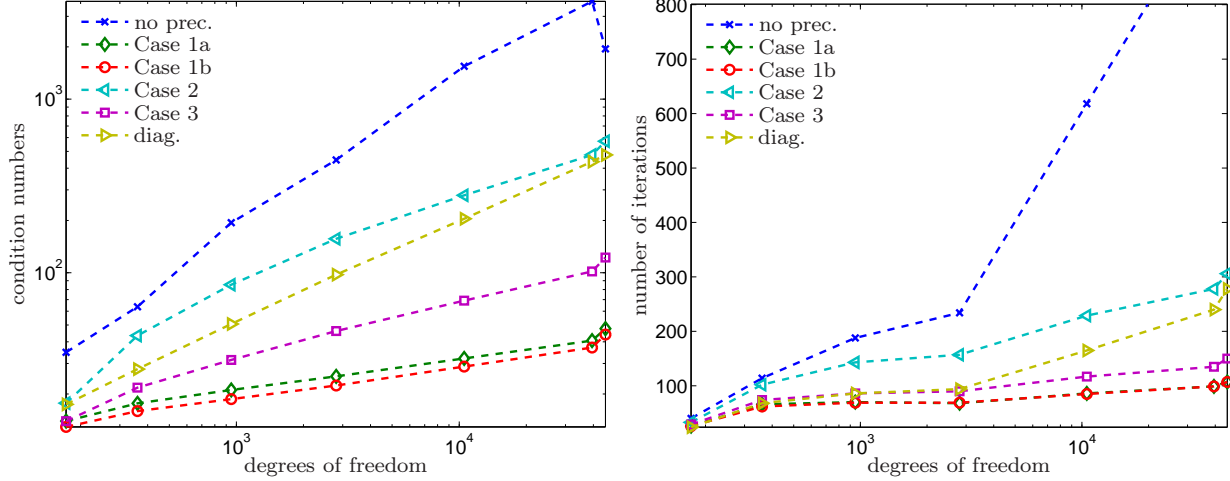


FIGURE 8. Condition numbers of the preconditioned systems and number of iterations in the MINRES algorithm for the example of Section 4.3 with different refinement levels of subdomain meshes.

step	dof	\underline{h}_1	\underline{h}_2	\underline{h}_3	\underline{h}_4	no prec.	1a	1b	2	3	diag.
1	172	1/4	1/6	1/6	1/4	34.77	13.97	12.94	17.72	13.96	17.43
2	360	1/4	1/12	1/6	1/8	63.62	17.67	15.95	43.41	21.77	27.83
3	948	1/4	1/24	1/12	1/8	194.24	21.10	18.70	85.29	31.43	50.64
4	2804	1/8	1/48	1/12	1/8	446.57	25.27	22.39	156.85	46.10	97.47
5	10532	1/8	1/96	1/24	1/16	1545.48	32.08	28.76	279.10	69.07	204.58
6	39492	1/16	1/192	1/24	1/32	3661.95	40.65	37.04	476.84	101.74	436.13
7	45316	1/32	1/192	1/48	1/64	1948.27	47.65	43.99	572.20	122.29	477.40

TABLE 3. Condition numbers of the preconditioned systems for the example of Section 4.3 with different refinement levels of subdomain meshes.

We consider uniform refinements where each element of \mathcal{T}_j is divided into four elements. For the experiment we refine each of the subdomain meshes separately, which leads to different mesh sizes $\underline{h}_1, \underline{h}_2, \underline{h}_3, \underline{h}_4$. Note that for our problem configuration there holds $h_j = \underline{h}_j$. The results are given in Figure 8 and Table 3. As in Section 4.2 we observe that the preconditioners P_{1a}, P_{1b} corresponding to the preconditioning form $d_1(\cdot, \cdot)$ behave best in terms of condition numbers and numbers of iterations. The preconditioners P_2 and P_3 stemming, respectively, from $d_2(\cdot, \cdot)$ and $d_3(\cdot, \cdot)$ show a stronger dependence on the mesh size. Nevertheless, theoretical bounds are confirmed also for this example. In particular, Figure 9 suggests that $\kappa(\tilde{\mathbf{C}}) \lesssim O(|\log(\underline{h})|^3)$ for all domain decomposition preconditioners.

Let us also remark that the condition number of the un-preconditioned system gets smaller from Step 6 to Step 7, see Table 3. The condition number $\kappa(\mathbf{C})$ is bounded (up to logarithmic terms) by $\lambda_{\max}^{1/2}/\lambda_{\min}$ and this term depends on the ratio $h^{1/2}/\underline{h}$. Since h gets smaller and \underline{h} stays constant from Step 6 to Step 7 (as we refine all subdomains except Γ_2), this explains the observation.

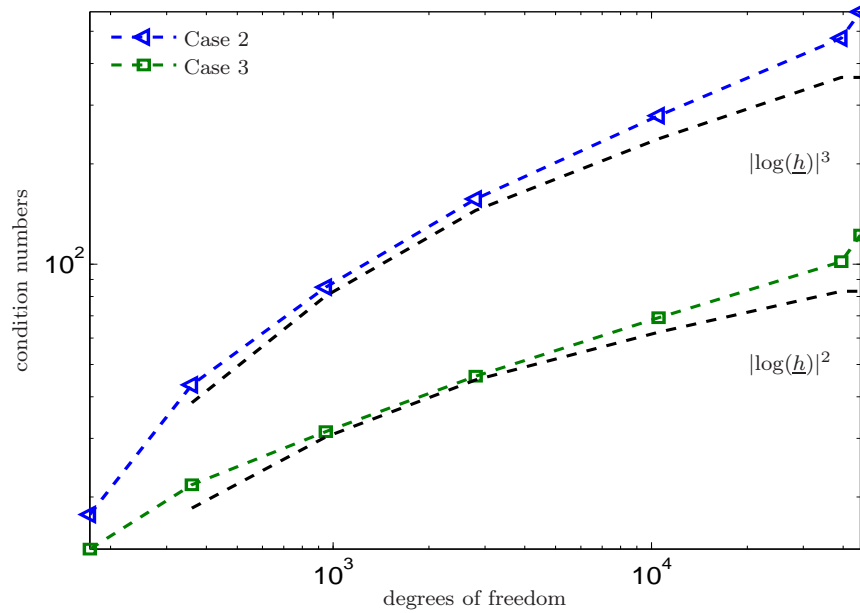


FIGURE 9. Logarithmic behavior of condition numbers for example of Section 4.3 with different refinement levels of subdomain meshes.

REFERENCES

- [1] Mark Ainsworth and William McLean. Multilevel diagonal scaling preconditioners for boundary element equations on locally refined meshes. *Numer. Math.*, 93(3):387–413, 2003.
- [2] Mark Ainsworth, William McLean, and Thanh Tran. The conditioning of boundary element equations on locally refined meshes and preconditioning by diagonal scaling. *SIAM J. Numer. Anal.*, 36(6):1901–1932, 1999.
- [3] Franz Chouly and Norbert Heuer. A Nitsche-based domain decomposition method for hypersingular integral equations. *Numer. Math.*, 121(4):705–729, 2012.
- [4] Catalina Domínguez and Norbert Heuer. A posteriori error analysis for a boundary element method with non-conforming domain decomposition. *Numer. Methods Partial Differential Eq.*, 30(3):947–963, 2014.
- [5] Maksymilian Dryja, Barry F. Smith, and Olof B. Widlund. Schwarz analysis of iterative substructuring algorithms for elliptic problems in three dimensions. *SIAM J. Numer. Anal.*, 31(6):1662–1694, 1994.
- [6] Michael Feischl, Thomas Führer, Norbert Heuer, Michael Karkulik, and Dirk Praetorius. Adaptive Boundary Element Methods. *Arch. Comput. Methods Engrg.*, 2014. Published online first June 2014.
- [7] Michael Feischl, Thomas Führer, Dirk Praetorius, and Ernst P. Stephan. Efficient additive Schwarz preconditioning for hypersingular integral equations. *ASC Report*, 25/2013, Vienna University of Technology, 2013.
- [8] Gabriel N. Gatica, Martin Healey, and Norbert Heuer. The boundary element method with Lagrangian multipliers. *Numer. Methods Partial Differential Equations*, 25(6):1303–1319, 2009.
- [9] Martin Healey and Norbert Heuer. Mortar boundary elements. *SIAM J. Numer. Anal.*, 48(4):1395–1418, 2010.
- [10] Norbert Heuer and Francisco-Javier Sayas. Crouzeix-Raviart boundary elements. *Numer. Math.*, 112(3):381–401, 2009.
- [11] Norbert Heuer and Ernst P. Stephan. Iterative substructuring for hypersingular integral equations in \mathbb{R}^3 . *SIAM J. Sci. Comput.*, 20(2):739–749, 1999.
- [12] Norbert Heuer and Ernst P. Stephan. An additive Schwarz method for the h - p version of the boundary element method for hypersingular integral equations in \mathbb{R}^3 . *IMA J. Numer. Anal.*, 21(1):265–283, 2001.

- [13] Norbert Heuer and Ernst P. Stephan. An overlapping domain decomposition preconditioner for high order BEM with anisotropic elements. *Adv. Comput. Math.*, 19(1–3):211–230, 2003.
- [14] Ralf Hiptmair, Carlos Jerez-Hanckes, and Shipeng Mao. Extension by zero in discrete trace spaces: Inverse estimates. Technical Report 2012-33, Seminar for Applied Mathematics, ETH Zürich, Switzerland, 2012.
- [15] Michael Karkulik, David Pavlicek, and Dirk Praetorius. On 2D newest vertex bisection: Optimality of mesh-closure and H^1 -stability of L_2 -projection. *Constr. Approx.*, 38:213–234, 2013.
- [16] Matthias Maischak. A multilevel additive Schwarz method for a hypersingular integral equation on an open curve with graded meshes. *Appl. Numer. Math.*, 59(9):2195–2202, 2009.
- [17] Matthias Maischak, Ernst P. Stephan, and Thanh Tran. Multiplicative Schwarz algorithms for the Galerkin boundary element method. *SIAM J. Numer. Anal.*, 38(4):1243–1268, 2000.
- [18] Alfio Quarteroni and Alberto Valli. *Domain Decomposition Methods for Partial Differential Equations*. Oxford University Press, 1999.
- [19] Torgeir Rusten and Ragnar Winther. A preconditioned iterative method for saddlepoint problems. *SIAM J. Matrix Anal. Appl.*, 13(3):887–904, 1992. Iterative methods in numerical linear algebra (Copper Mountain, CO, 1990).
- [20] Barry Smith, Petter Bjørstad, and William Gropp. *Domain Decomposition*. Cambridge University Press, 1996.
- [21] Olaf Steinbach and Wolfgang L. Wendland. The construction of some efficient preconditioners in the boundary element method. *Adv. Comput. Math.*, 9(1-2):191–216, 1998. Numerical treatment of boundary integral equations.
- [22] Ernst P. Stephan. Multilevel methods for the h-, p- and hp-versions of the boundary element method. *J. Comput. Appl. Math.*, 125:503–519, 2000.
- [23] Ernst P. Stephan and Thanh Tran. Domain decomposition algorithms for indefinite hypersingular integral equations – the h- and p-versions. *SIAM J. Sci. Comput.*, 19(4):1139–1153, 1998.
- [24] Andrea Toselli and Olof Widlund. *Domain decomposition methods—algorithms and theory*. Springer-Verlag, Berlin, 2005.
- [25] Thanh Tran. Overlapping additive Schwarz preconditioners for boundary element methods. *J. Integral Equations Appl.*, 12(2):177–207, 2000.
- [26] Thanh Tran and Ernst P. Stephan. Additive Schwarz methods for the h -version boundary element method. *Appl. Anal.*, 60(1-2):63–84, 1996.
- [27] Andrew Wathen, Bernd Fischer, and David Silvester. The convergence rate of the minimal residual method for the Stokes problem. *Numer. Math.*, 71(1):121–134, 1995.

FACULTAD DE MATEMÁTICAS, PONTIFICIA UNIVERSIDAD CATÓLICA DE CHILE, AVENIDA VICUÑA MACKENNA 4860, SANTIAGO, CHILE

E-mail address: {tofuhrrer,nheuer}@mat.puc.cl